Phase diagram of bosonic hard rods in a one dimensional optical lattice

F. De Soto and M.C. Gordillo
Departamento de Sistemas Físicos Químicos y Naturales,
Universidad Pablo de Olavide. 41013 Sevilla, Spain

We calculated the phase diagram of a pure one dimensional (1D) system of hard rod bosons when it is loaded in optical lattices of different depths by means of a Diffusion Monte Carlo (DMC) technique. The results were compared with those for a Bose-Hubbard model for the same range of densities and characteristic parameters. Both diagrams were found to be qualitatively similar in the regime in which a one-band Hubbard model is adequate, being that comparison poorer when this condition is not fulfilled.

PACS numbers: 05.30.Jp, 67.85.-d

INTRODUCTION

After the production of the first Bose-Einstein condensates in dilute alkali atom clouds [1–3], one of the most interesting developments in the field is the confining of these atoms in what are called optical lattices [4]. These are an array of potential wells created by making two coherent lasers interfere to generate an standing wave whose periodicity in the direction of the beams is $\lambda/2$, being λ the wave length of the chosen light. The trapping of the neutral atoms in these energy minima is due to the induction of an oscillating dipole moment that allows it to interact with the electrical field of the laser light [5] and "feel" the potential well.

The interference of two lasers produce a set of quasi two dimensional flattened up dilute gas clouds. If another couple of beams is switched on perpendicularly to the first ones, a series of elongated cigars are produced [6]. The degree of confinenement in both directions could be varied experimentally to create something very close to a 1D system [7, 8]. In Ref. [8] a further degree of atom constraining was imposed by introducing a third pair of lasers in the direction of main axis of the cylinder. This produced an 1D optical lattice, in which the ^{87}Rb atoms see an array of potential wells whose depth could be manipulated to change the properties of the system. Our aim in this work is to describe these kind of elongated 1D arrangements by using a continuous Hamiltonian instead of the discrete approximations that comprise the majority of the literature. See for instance Ref. 9 and references therein.

The most general type of these one dimensional Hamiltonians can be described by the expression:

$$H = -\frac{\hbar^2}{2m}\sum_{i=1}^{N}\left[\frac{\partial^2}{\partial z^2} + V_{ext}(z_i)\right] + \sum_{i<j} V(z_{ij}) \qquad (1)$$

in which we have assumed that the particles are located along the z axis. z_{ij} is then the distance between the particles i and j, of coordinates z_i and z_j along that axis. $V_{ext}(z_i)$ is the external potential at each z coordinate. For an optical lattice confining potential in three dimensions we will have:

$$\begin{aligned} V_{ext}(x_i, y_i, z_i) &= \sum_{i=1}^{3} V_{0,1}\sin^2(k_1 x_i) + \\ &+ V_{0,2}\sin^2(k_2 y_i) + V_{0,3}\sin^2(k_3 z_i) \end{aligned} \qquad (2)$$

where $k_{1,2,3}$, are the wavenumbers $(2\pi/\lambda)$ of the confining lasers. If the particles are tightly bounded in the two directions perpendicular to the z axis, the $\sin(k_1 x_i)$ and $\sin(k_2 y_i)$ functions can be developed around $x_i = 0$ and $y_i = 0$ respectively, to obtain:

$$V_{ext}(x_i, y_i) = V_{0,1}(k_1 x_i)^2 + V_{0,2}(k_2 y_i)^2 \qquad (3)$$

and if the system is symmetric in the change $x \leftrightarrow y$, then, $V_{0,1} = V_{0,2} := V_{0,\perp}$, $k_1 = k_2 = k_\perp$ and $x_i^2 + y_i^2 = r_\perp^2$, allowing us to write:

$$V_{ext}(x_i, y_i, z_i) = V_{0,3}\sin^2(k_3 z_i) + V_{0,\perp}(k_\perp r_{i\perp})^2 \qquad (4)$$

i.e., we end up with the equivalent of a 1D optical lattice and a perpendicular harmonic confinement. If this confinement is such that movement in the radial direction is greatly impeded, one can safely assume that the neutral atoms are frozen in the ground state of the harmonic trap, and use that contribution ($NV_{0,\perp}k_\perp^2$, N, number of particles in the system), as the zero of the energy scale. We have then (making $V_{0,3} = V_0$):

$$V_{ext}(z_i) = V_{0,3}\sin^2(k_3 z_i) = V_0\sin^2(k z_i) \qquad (5)$$

To complete the definition of the model, we have to give a particular form for the interparticle potential $V(z_i - z_j)$. A very common approximation [10–17] , and the one we will use here, is to consider the atoms as hard rods (the 1D counterpart of the hard spheres), i.e., $V(z_{ij}) = +\infty$ if $|z_i - z_j| < a$, being a the diameter of the hard rod which corresponds here to the s-wave scattering length. When no optical lattice potential is present, this model is exactly solvable [13, 18].

The plan of the paper is as follows. In section II, we will describe the method we used to solve the equations that describe the system of bosons. In section III we will

show the results obtained in several density and interaction regimes, concluding by displaying a phase diagram for densities less than two atoms per potential well of the optical lattice. Section IV will be devoted to the comparison of these results with that of the one-band Bose-Hubbard model for strictly 1D systems. We will close with a summary and conclusions.

METHOD

To solve the Hamiltonian given in Eq. (1). we used a Diffusion Monte Carlo (DMC) algorithm. This well-known technique give us the exact energy of the ground state of a system of interacting bosons within some controllable statistical uncertainties [19]. This means that we are exactly at T =0 K, what is expected to be a good approximation in this context, given the very low temperatures used in the optical lattice studies. To use this method, we have to define what it is called a *trial function*,i.e., an approximation to the real wave function that allows us to perform an importance sampling instead of a completely random exploration of the phase space (see further details in Ref. 19). The *trial function* should be different of zero in the regions in which there can be particles, and zero otherwise. The function used in this work was of the form:

$$\Phi(z_1, z_2, ..., z_N) = \prod_{i=1}^{N} \psi(z_i) \prod_{j<k=1}^{N} f(z_{jk}) \qquad (6)$$

Here, $\psi(z_i)$ tends to localize the particles in the wells created by the 1D optical lattice, having as many maxima and minima as the number of these potential wells. It was obtained by numerically solving the Schroedinger equation corresponding to the Hamiltonian of Eq. (1) but considering only one particle loaded in the 1D optical lattice. The value of $\psi(z_i)$ at its minima decreases when V_0 increases.

$f(z_{kj})$ is a two body form analogous at the Jastrow expression used widely in condensed matter calculations [19]. We used for convenience the numerical solution of a purely 1D system of two hard rods when V_0= 0. This is completely equivalent to use the analytical solution [13] for this arrangement, since, in absence of the optical lattice potential, we checked that the different between the energy obtained and the exact one given by:

$$\frac{E}{N} = \frac{\hbar^2}{2m}\frac{\pi^2}{3}\frac{n^2a^2}{1-n^2a^2} \qquad (7)$$

was less than a part in a thousand. Here, n is the density of the hard rods, m its mass, and a its length. N is the total number of particles.

Experimentally, an important magnitude is the recoil energy, $E_R = \frac{\hbar^2k^2}{2m}$, that is a natural unit to define the energy of the system. In this work, we will use that scale and give our results in units of E_R. The other two remaining parameters to describe the problem are the length of the hard rods, a, and the wavelength of the laser, λ, that sets the periodicity of the optical lattice as $\lambda/2$. As defining a as the unit of length, we have only to define the ratio λ/a. Experimentally, it could vary from ~ 40 to ~ 150 (see for instance Refs. 8, 20–22 as examples of ^{87}Rb and ^{133}Cs atoms trapped in different optical lattices). In this work, we fixed $\lambda/a = 50$. Other ratios gave the same qualitative results and will be not presented here. We simulated systems with filling fractions (number of particles per potential well) between 0 and 2. To do so, we fixed $N = 30$, and changed the length of the simulation cell accordingly (i.e., for a filling fraction of 0.5, we used a simulation cell with 60 minima, and length $1500a$). The use of cells containing 60 atoms for the same densities did not change the simulation results.

RESULTS

In Figs. (1) and (2), we show the dependence of the energy per particle, in units of E_R, as a function of the depth of the potential well, for the V_0's given in the insets. The exact solution, for V_0= 0 (Eq. (7) above), is also displayed for comparison. The trend for small confinement is what one would expect: the energy per particle increases with respect to the homogeneous unconfined gas in an amount that for low V_0 is basically (but not completely, see below) constant for the density range considered. This is what we see for V_0 =0.32 E_R in Fig. (1). On the other hand, when the external potential is tuned up, the slope of the energy starts to develop a discontinuity at a filling fraction of one ($n\lambda/2 = 1$). This is true even for the smallest confinement, as the dashed lines show. These curves are polynomial fits to the energy results above and below the density $n\lambda/2$ =1, and are intended as guides-to-the-eye.

The dependence of the energy with the density for large values of V_0 in shown in Fig. (2) and can be understood in a simple way: when the filling fraction is smaller than one, each particle remains confined in one well and the energy per particle does not grow with the addition of more particles (dashed lines up to $n\lambda/2 = 1$ in Fig. (2). When there is already one particle in each well, each additional atom adds an energy $\epsilon + U$, where ϵ is the energy of one particle in one cell, and U the increase of energy due to the interaction between hard rods. In a system with N particles and C cells, the total energy when $C < N < 2C$ shall be:

$$E = C\epsilon + (N - C)(\epsilon + U) \ , \qquad (8)$$

i.e., ϵ for every cell and additionally $\epsilon + U$ for cells containing two particles. This implies that the energy per

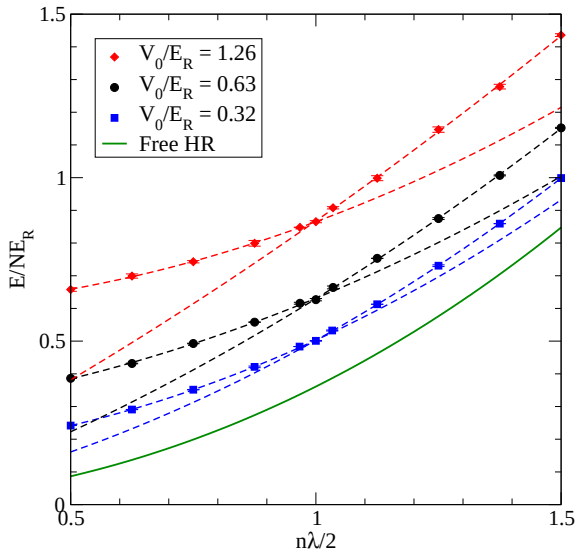

FIG. 1: *(Color online) Energy per particle (in units of E_R) versus the filling fraction for small V_0. Lines correspond to a fit above and below filling fraction one and are meant as mere guides-to-the-eye.*

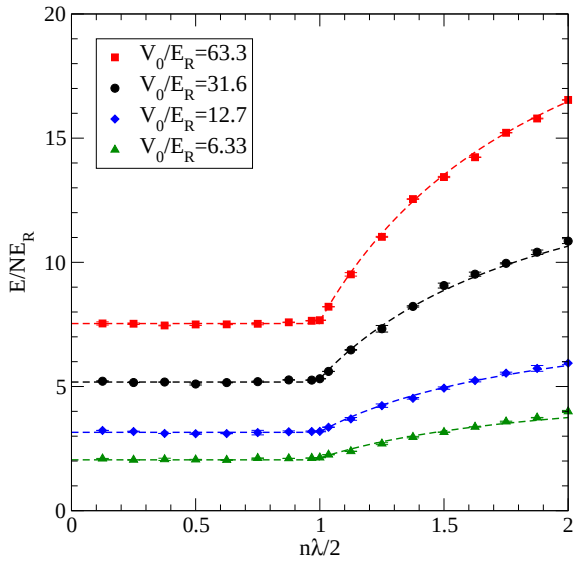

FIG. 2: *(Color online) Energy per particle (in units of E_R) vs the filling fraction for large values of V_0. Lines are a fit to a phenomenological model described in the text. Simulation results are displayed as symbols.*

particle depends on the density $n = \frac{N}{C\lambda/2}$as:

$$\frac{E}{N} = \epsilon + U\left(1 - \frac{1}{n\lambda/2}\right) \tag{9}$$

for filling fractions between one and two ($1 \leq n\lambda/2 \leq 2$).

This dependence is indeed found in the numerical DMC calculations. In Fig. (2), the energies obtained numerically have been plotted vs n for different values of V_0/E_R. The dependence predicted by expression in Eq. (9) is shown by the dashed lines, and reproduce accurately the dependence of the energy with n for $n\lambda/2 > 1$.

From the data of Figs. (1) and (2) above, we can obtain the chemical potential of the system as a function of the density, n. At zero temperature and in units of E_R:

$$\frac{\mu}{E_R} = \frac{\partial \frac{E}{E_R}}{\partial N} = n\frac{\partial \frac{E}{NE_R}}{\partial n} + \frac{E}{NE_R} \tag{10}$$

where E is the total energy of the system and N is the number of particles. At exactly $n\lambda/2 = 1$, we observe a discontinuity in μ/E_R, since the chemical potential is different when we approached that point from bigger or smaller densities. This corresponds to the change in the energy slope at $n\lambda/2 = 1$ in Figs. (1) and (2). This change is similar to the obtained in the numerical treatment of the one-dimensional Bose-Hubbard model in Refs. 9, 23, 24. Following exactly the same procedure used in those works, we defined the boundaries of the Mott insulator phase as the values of the chemical potential at the edges of the plateaus of the corresponding density vs. chemical potential curves. A representative example of those curves is shown in Fig. (3). In our case, the gap in the chemical potential when the filling fraction equals one depends on the magnitude of the confining potential V_0 of the particular optical lattice considered. If we plot these upper and lower values of μ/E_R as a function of V_0/E_R, we have the phase diagram of Fig. (4).

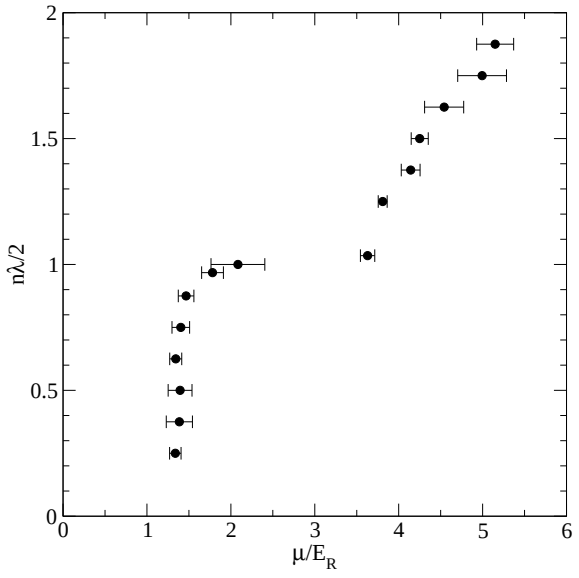

FIG. 3: *Filling fraction as a function of the chemical potential for an optical lattice with V_0/E_R= 3.2 .*

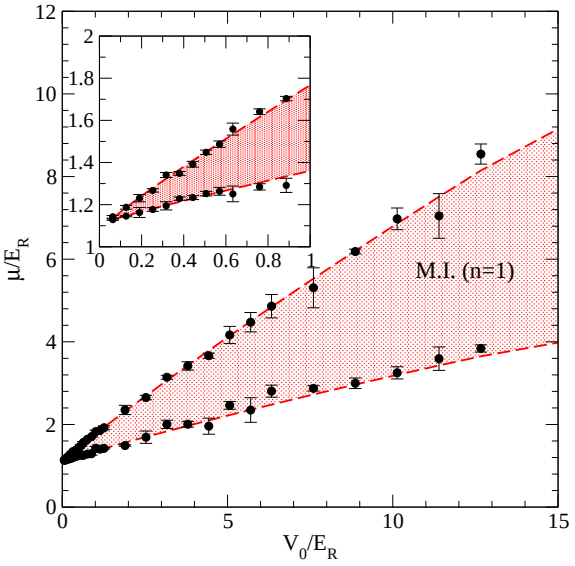

FIG. 4: *(Color online) Mott insulating phase diagram for a 1D optical lattice. Black circles correspond to the chemical potential obtained numerically below and above $n\lambda/2 = 1$. Lines are mere guides-the-eye. An onset shows with more detail the cases of small V_0.*

There, the shadowed region corresponds to the MI phase, being the unshadowed one a gas. In Fig. (4) we display only the part of the diagram corresponding to densities lower than two atoms per potential well. One would expect another MI region to appear for the values of μ/E_R and V_0/E_R compatible with a filling fraction of two. This is what usually is displayed in a Bose-Hubbard model description of the system [25]. A great advantage of this continuous model with respect to that Bose-Hubbard one is that depends on magnitudes that are directly comparable to experiment, as V_0 and E_R instead of more convoluted parameters as J and U (see below). For instance, from Fig. (4), one is able to say that, in a pure 1D system, there is not a MI phase for V_0/E_R values less that ~ 0.5. This is the point at which the two μ/E_R values around $n\lambda/2$=1 are compatible within their respective error bars.

COMPARISON WITH A BOSE-HUBBARD MODEL

There is a huge literature on the Bose-Hubbard model applied to optical lattices in general and to a 1D optical lattices in particular (see for instance, Refs. [6, 9] and all the references therein). This is a discrete model, that can be derived from a continuous Hamiltonian after a series of simplifications. The first one is that the atoms can be only at the minima of the potential wells of the optical lattice, being that minima the sites of the Bose-Hubbard model lattice. In addition, we suppose that the wave function of the system can be written as a product functions that depend only of the coordinates of a single particle, i.e.:

$$\Phi(z_1, z_2, ..., z_N) = \prod_{i=1}^{N} \psi(z_i) \tag{11}$$

where each $\psi(z_i)$ could be developed in a basis of Wannier functions. This equation is a particular case of Eq. (6) when $f(z_{jk}) = 1$ for all pairs kj. If we keep only the functions corresponding to the lowest vibrational states of the particle in each well, we have:

$$\psi(z) = \sum_i w_i(z - z_i) b_i \tag{12}$$

where b_i is the second quantization operator that annihilates a particle localized at lattice site i. Under this set of approximations, the Hamiltonian in Eq. (1) turns into [26]:

$$H = -J \sum_{\langle ij \rangle} b_i^\dagger b_j + \frac{U}{2} \sum_i n_i(n_i - 1) + \sum_i \epsilon_i n_i \tag{13}$$

where $\langle \cdots \rangle$ stands for the closest neighbors and $b_i^\dagger(b_i)$ are the creation (annihilation) operators for a boson at lattice site i. The parameters J, U and ϵ_i depend on the interaction terms of the primitive Hamiltonian. In particular:

$$J_{ij} = -\int dz \;\; w_i^*(z) \left[-\frac{\hbar^2}{2m} \frac{\partial^2}{\partial z^2} + V_{ext}(z) \right] w_j(z) \tag{14}$$

This means that the parameter $J = J_{\langle ij \rangle}$ can be calculated by obtaining numerically the exact Wannier functions without any further approximation [27] . The dependence of the parameter J obtained in this way with the potential depth V_0 is represented in Fig. (5) as a solid line. If instead of the exact Wannier functions we use Gaussians centered at potential minima, we have this analytical expression [6]:

$$\frac{J}{E_R} = \frac{4}{\sqrt{\pi}} E_R \left(\frac{V_0}{E_R} \right)^{3/4} \exp \left[-2 \left(\frac{V_0}{E_R} \right)^{1/2} \right] \tag{15}$$

which has been plotted in Fig. (5) (dashed line) for comparison. As expected, the approximate value given by Eq. (15) coincides with the exact one for large values of V_0 but differs significatively for small values of V_0. The parameter ϵ_i is simply J_{ii} and represents the characteristic energy of a particle confined in a potential well. In an inhomogeneous unconfined system, each well could have a different in-site energy, in that case ϵ_i would be different for each i, instead of the usual case in which for all sites we can define a common $\epsilon = \epsilon_i$.

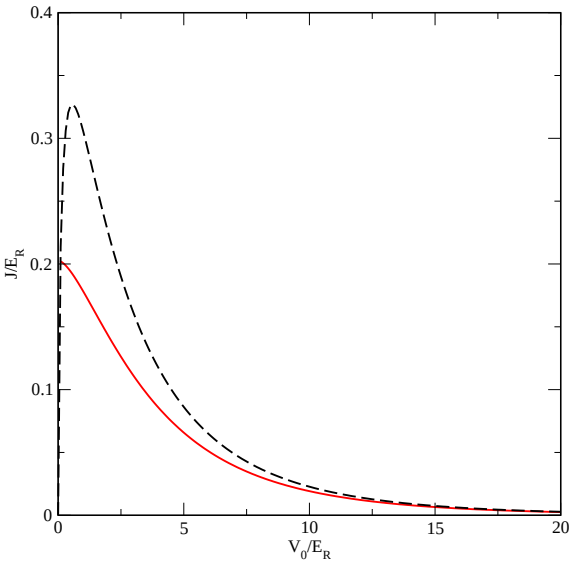

FIG. 5: *(Color online) Parameter J vs the external potential depth V_0 in units of the recoil energy E_R, calculated by numerical evaluation of Eq. (14) –solid line– and analytical result given by Eq. (15) –dashed line–.*

In the Bose-Hubbard Hamiltonian, the term that takes into account the interaction between particles in the same lattice site is U. With the same approximations than before:

$$U = -\int dz dz' \; w_i^*(z) w_j^*(z') V_{ext}(z-z') w_k(z) w_l(z) \quad (16)$$

that goes to infinity wherever $z - z'$ is smaller than the hard rod length. This means that one cannot in truth use a Bose-Hubbard model to describe a purely 1D system of hard rods. A way out of this predicament could be to use the approach of Olshanii [28] that considers a quasi one dimensional system of three dimensional spheres and produces an expression for U than depends on $\omega_\perp$, the transverse harmonic confining frequency [6]. However, that is not a pure 1D system directly comparable with our calculations here.

Since we want to compare our results to the ones for pure 1D Bose-Hubbard models in the literature [9, 25] we have to devise a practical method to compute U in our system of hard rods. In the Bose-Hubbard Hamiltonian, U is the additional energy we have when we added a particle to a site that it is already populated. If in Eq. (13), we had only one lattice site and two particles on it, the total energy would be $E_2 = 2\epsilon + U$. On the other hand, if we had only one particle in this same site, the total energy will be only ϵ. This means that we can estimate U as:

$$U = E_2 - 2\epsilon \quad (17)$$

This is what we made, computing ϵ and E_2 as the corresponding energies of one and two hard rods in a 1D optical lattice with only one potential minimum. The results are given in Fig. (6) for different values of V_0.

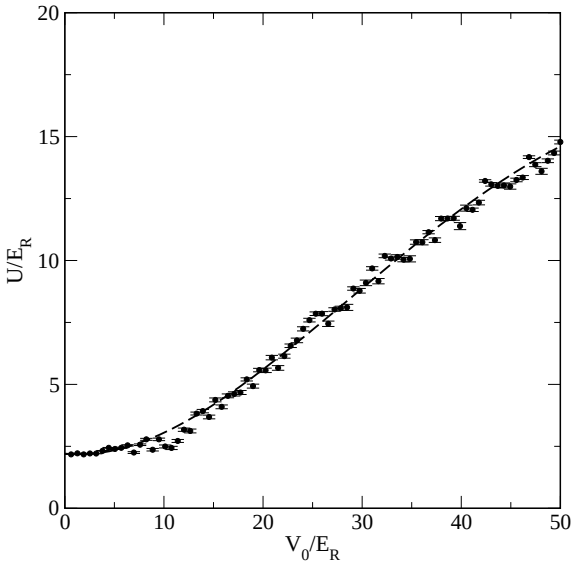

FIG. 6: *(Color online) Estimation of the value of the parameter U in the Bose-Hubbard model for a system of hard bosons vs the external potential depth, V_0, both of them in units of the recoil energy .*

With the parameters J and U so obtained, we can translate our phase diagram in Fig. (4) to the language used for the Bose-Hubbard model. For each value of V_0, we have the two μ values that limit the MI phase in Fig. (4). With the help of Figs. (5) and (6) we obtain the J and U values corresponding to that V_0, and display μ/U as a function of J/U in Fig. (7). The shadowed zone is the transposition of its counterpart in Fig. (4), and the dashed lines are the limits of the MI phase for a pure 1D Bose-Hubbard model as calculated numerically and presented in Ref. 9 and references therein. We can see that the differences between the results derived form this work and the values in the literature are bigger in the case of high J/U values, i.e. for the case of small V_0's (from Figs. (5) and (6) is easy to deduce that when $V_0 \to 0$, J is bigger and U smaller). It is exactly for these small values of V_0 that one expects the Bose-Hubbard model to perform worst, since when the potential wells of the optical lattices are shallow, the approximation of using only the Wannier functions corresponding to the first band gets poorer. On the other hand, in the limit $J/U \to 0$ (for big V_0's), the agreement is good, in concordance with the soundness of using the approximations involved in the derivation of the Bose Hubbard model for these cases.

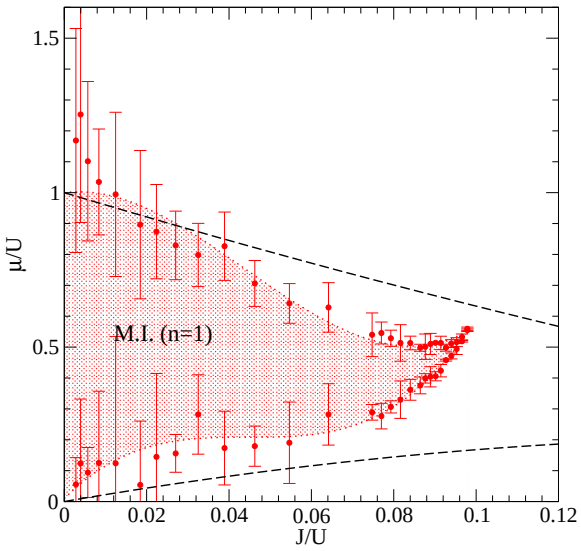

FIG. 7: *(Color online) Phase diagram of the optical lattice expressed in terms of the parameters J and U of a 1D Bose-Hubbard model.*

CONCLUSIONS

We presented DMC calculations for the energy and the Mott-insulator phase diagram of a 1D system of hard rods loaded in optical lattices of different depths, represented by the V_0 parameter. We found that for high V_0's the energy of the system could be described by a simple expression relative to the number of wells occupied by one and two atoms. We can see also that there is sizeable discontinuity in μ/E_R for a filling fraction of one, even for small values of V_0. However, if $V_0 < 0.5$ the discontinuity is smoothed out and the gas does not change to a Mott insulator at $n\lambda/2 = 1$. We also compared our Mott insulator phase diagram with the one obtained for a pure 1D Bose-Hubbard model. We found that both descriptions are similar to each other when the approximations used to derive the discrete Hamiltonian are reasonable, i.e. for deep potential wells. In other cases, both phase diagrams are noticeably different.

We acknowledge partial financial support from the Junta de Andalucía group PAI-205 and grant FQM-5985, DGI (Spain) grant No. FIS2010-18356.

[1] M.H. Anderson, J.R. Ensher, M.R. Mathews, C.E. Wieman and E.A. Cornell. Science. **269** 389 (1995).
[2] C. C. Bradley, C. A. Sackett, J. J. Tollett, and R. G. Hulet Phys. Rev. Lett. **75** 1687 (1995).
[3] K. B. Davis, M. O. Mewes, M. R. Andrews, N. J. van Druten, D. S. Durfee, D. M. Kurn, and W. Ketterle Phys. Rev. Lett. **75** 3969 (1995).
[4] M. Greiner and S. Fölling. Nature (London) **453** 736 (2008).
[5] I. Bloch. Nat. Phys. **1** 23 (2005).
[6] I. Bloch, J. Dalibard and W. Zwerger Rev. Mod. Phys. **80** 885 (2008).
[7] T. Kinoshita, T. Wenger and D. S. Weiss. Science **305** 1125 (2004).
[8] B. Paredes, A. Widera, V. Murg, O. Mandel, S. Fölling, I. Cirac, G.V. Shlyapnikov, T.W. Hänsch and I. Bloch. Nature (London) **429** 277 (2004).
[9] M.A. Cazalilla, R. Citro, T. Giamarchi, E. Orignac and M. Rigol arXiv:1101.5337v1. (2011).
[10] J.L. DuBois and H.R. Glyde. Phys. Rev. A **63** 023602 (2001).
[11] G. E. Astrakharchik and S. Giorgini. Phys. Rev. A **66** 053614 (2002).
[12] D. Blume. Phys. Rev. A **66** 053613 (2002).
[13] F. Mazzanti, G.E. Astrakharchik, J. Boronat and J. Casulleras. Phys. Rev. Lett. **100** 020401 (2008).
[14] P. Grüter, D. Ceperley and F. Laloë. Phys. Rev. Lett. **79** 3549 (1997).
[15] M.C. Gordillo and D.M. Ceperley **85** 4735 (2000).
[16] S. Giorgini, J. Boronat and J. Casulleras. Phys. Rev. A **60** 5129 (1999).
[17] F. Mazzanti, A. Polls and A. Fabrocini. Phys. Rev. A **67** 063615 (2003).
[18] T. Nagamiya. Proc. Phys. Math. Soc. Jpn. **22** 705 (1940).
[19] J. Boronat and J. Casulleras, Phys. Rev. B **49**, 8920 (1994).
[20] S. Fölling, S. Trotzky, P. Cheinet, M. Feld, R. Saers, A. Widera, T. Müller and I. Bolch. Nature (London) **448** 1029 (2007).
[21] N. Gemelke, X. Zhang, C.L. Hung and C. Ching. Nature (London) **460** 995 (2009).
[22] W.S. Bakr, J.I. Gillen, A. Peng, S. Fölling and M. Greiner **462** 74(2009).
[23] G. G. Bratouni, R.T. Scalettar and G.T. Zimanyi. Phys. Rev. Lett. **65** 1765 (1990).
[24] G. G. Bratouni and R.T. Scalettar. Phys. Rev. B **46** 9051 (1992).
[25] C. Kollath, U. Schollwöck, J. von Delft and W. Zwerger. Phys. Rev. A. Rapid communications. **69** 031601 (2004).
[26] D. Jaksch, C. Bruder, J.I. Cirac, C.W. Gardiner and P. Zoller. Phys. Rev. Lett. **81** 3108 (1998).
[27] M. Abramowitz and I.A. Stegun. Hasndbook of Mathematical functions. Dover, New. York. (1965).
[28] M. Olshanii. Phys. Rev. Lett. **81** 938 (1998).